

Supplementary Information

Fast Purcell-enhanced single photon source in 1,550-nm telecom band from a resonant quantum dot-cavity coupling.

Muhammad Danang Birowosuto¹, Hisashi Sumikura¹, Shinji Matsuo², Hideaki Taniyama¹, Peter J. van Veldhoven³, Richard Nötzel^{3,#}, Masaya Notomi^{1,a}

- 1) NTT Basic Research Laboratories, NTT Corporation, 3-1 Morinosato Wakamiya, Atsugi, Kanagawa 243-0198, Japan
- 2) NTT Photonics Laboratories, Corporation, 3-1 Morinosato Wakamiya, Atsugi, Kanagawa 243-0198, Japan
- 3) COBRA Research Institute, Eindhoven University of Technology, Postbus 513, 5600 MB Eindhoven, The Netherlands

[#] Present address: Institute for Systems based on Optoelectronics and Microtechnology (ISOM), ETSI Telecommunication, Technical University of Madrid, Ciudad Universitaria s/n, 28040, Madrid, Spain

^a Email: masaya.notomi@lab.ntt.co.jp

1. Exciton (X) and biexciton (XX) of single quantum dot (QD) in the reference samples

Fig. S1(a) shows the photoluminescence (PL) spectra of the quantum dot (QD) inside a reference sample recorded at 4 K. In this sample, we observed the exciton (X) and biexciton (XX) peaks at 1,557 and 1,561 nm, respectively. The XX line is 2 meV above the X line. Such “antibinding” of the XX state in InAs/InP QD was previously reported [1]. The full width half maximum (FWHMs) of the X and XX lines are 0.47 and 0.49 nm, respectively. These values are slightly larger than the resolution of the spectrometer of 0.39 nm. The integrated intensities of the X and XX lines have linear and quadratic behavior, respectively, see Fig. S1(b). In Fig. 3 of the manuscript, we also confirmed the X and XX lifetimes of 1.6 and 1 ns, respectively, which correspond to the calculated radiative recombination of X and XX in InAs/InP QD [2].

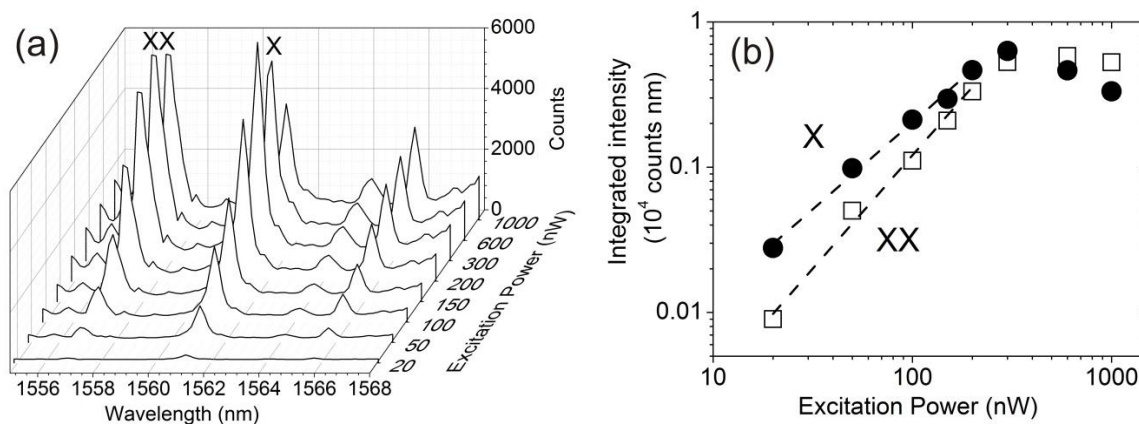


Fig. S1(a) Photoluminescence (PL) spectra of exciton (X) and biexciton (XX) of quantumdots (QDs) as a function of excitation powers at 4 K. (b) Integrated intensities of X and XX lines as a function of CW laser power.

2. X and XX of single QD and the cavity in the photonic crystals

We changed the lattice constant of the photonic crystals for tuning the cavity emission to the 1,550-nm QDs emission. PL spectra of QDs inside a cavity of photonic crystals recorded at 4 K are presented in Fig. S2. Fig. S2 shows the shift of the fundamental cavity as a function of lattice constant. The shift is from 1,402 to 1,558 nm and it well agrees with the FDTD calculations. We observed the same X and XX lines as previously observed in the reference sample for the photonic crystal nanocavity with a lattice constant of 440 nm, see Fig. S3(a). This figure shows the temperature dependence of PL spectra of the cavity, X and XX lines. The X and XX lines shift to longer wavelength along with the increase of the temperature. At the first sight, both shifts of the X and XX lines in the cavity are the same with those in the reference sample. This shift of the peak center, the peak width and the integrated intensities are depicted in Fig. S3(b). The peak centers of X and XX lines in the cavity are at the same wavelength with those in the reference sample. However, for the peak widths of the XX in the cavity, we only collect those which the XX is off resonance. The peak widths of the X and the XX lines in the cavity are the same with those in the reference sample. The integrated intensities as a function of temperatures show that the intensities of the XX emission start to increase when it is close to zero detuning.

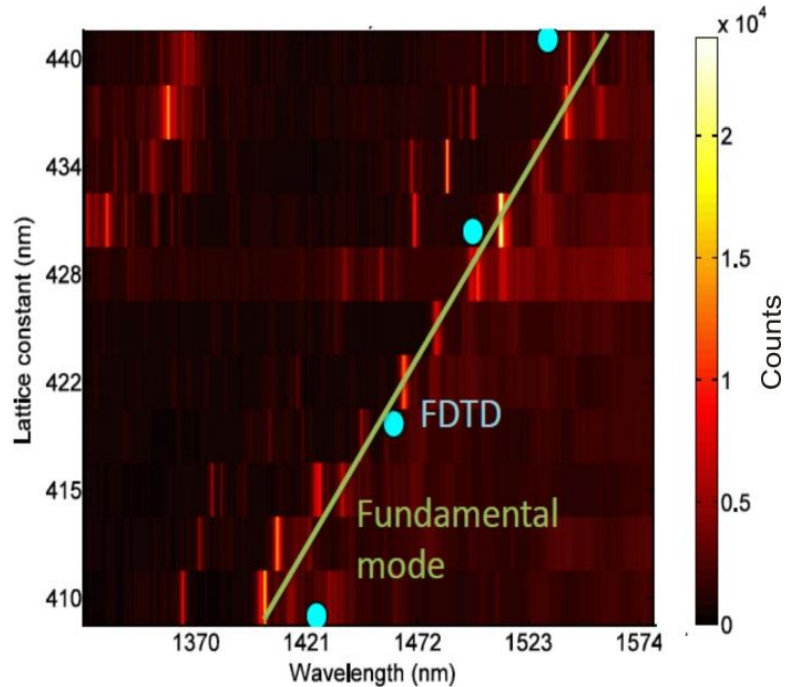


Fig. S2 Photoluminescence (PL) spectra of quantum dots (QDs) inside the line-defect cavity as a function of lattice constant. The yellow line is a guide to the cavity peaks (fundamental mode) whereas the blue dots are the cavity peaks from finite difference time domain (FDTD) calculation.

3. Inhibition of the spontaneous emission of XX of single QD in photonic band gap.

In the manuscript, we observed the shortening of the XX lifetime in the cavity at zero detuning. For a proof that this shortening is due to the Purcell effect, we measured time-resolved emission of XX QD from the other type of cavity (L3; three-missing-hole cavity and the lattice constant of the photonic crystal is 420 nm) and this photonic crystal are still in the same sample with that of line-defect cavity. From the PL spectrum in Fig. S4(a), the cavity and the XX emissions are observed at 1,440 and 1,557 nm, respectively. Both emissions were separated by ~ 120 nm, which means the XX are completely off resonance. The XX emission is also ~ 45 nm far from the bandgap edge. Unlike the width-modulated line-defect cavity which XX emission may still be enhanced by the line-defect [3], the XX emission in L3 cavity is inhibited by the photonic bandgap [4].

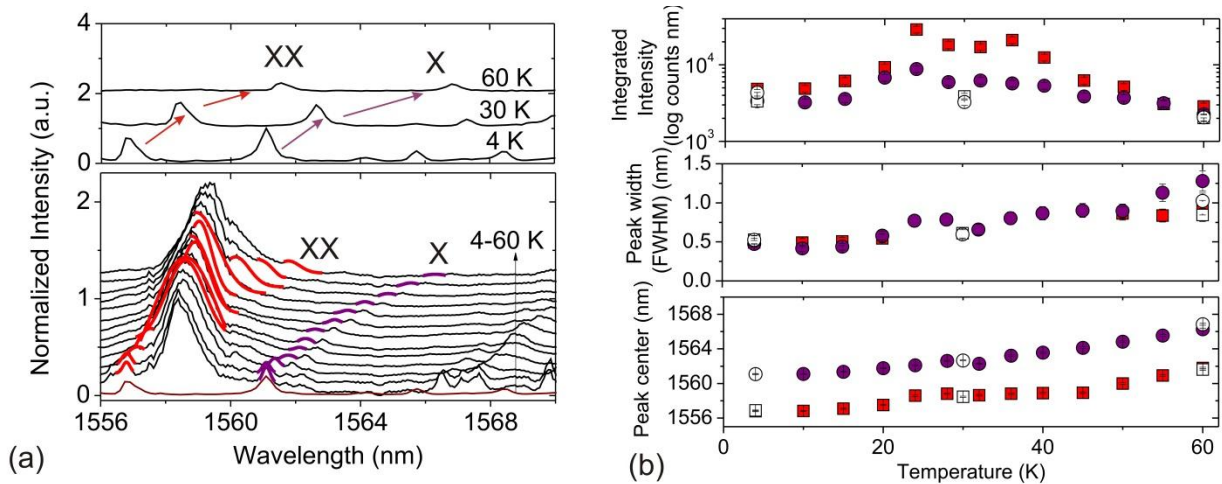


Fig. S3(a) Normalized photoluminescence (PL) spectra of QDs inside the reference samples (top) and the line-defect cavity (bottom) as a function of temperatures. The red and purple lines in the PL spectra are to guide X and XX, respectively. The brown line is the PL spectrum in the reference sample at 4K. (b) Peak center, width and integrated intensity of X (purple circles) and XX (red squares) in the cavity derived from the raw PL spectra. Those for X and XX in the reference samples are shown by empty circles and squares, respectively.

Fig. S4(b) shows the time-resolved emission of the XX emission in the L3 cavity. The single-exponential is good for the fit analysis of the curve, see residual curve in Fig. S4b. The fit yields a lifetime of 2.2 ns. The inhibition factor calculated from the lifetime of XX in reference sample is therefore 2.2 times. In comparison with the recent observation of the inhibition of the spontaneous emission of InGaAs QD in the same structure of the 2D photonic crystal [5], the inhibition corresponds well with that measured with total decay rates at the same frequency and the calculated LDOS.

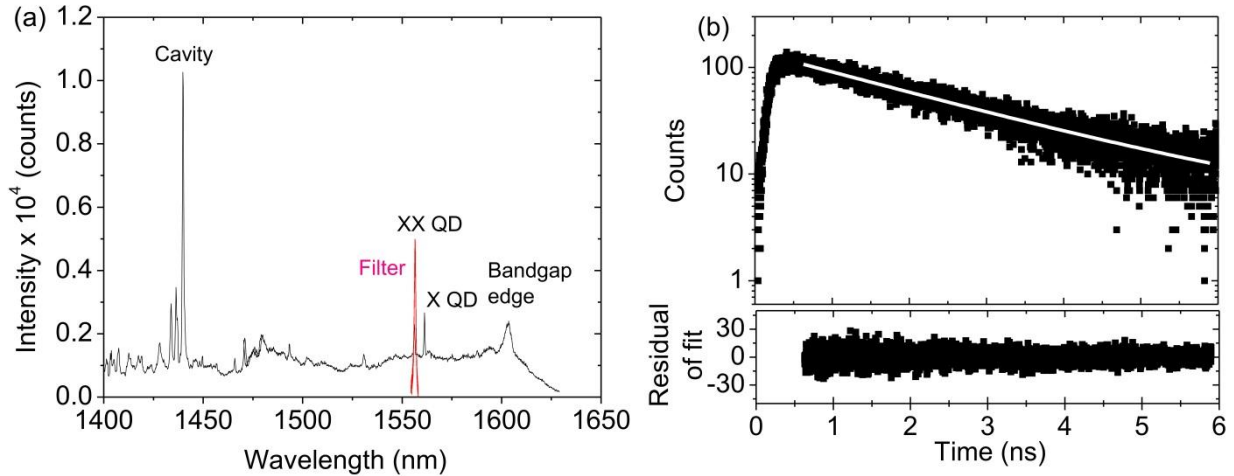


Fig. S4(a) Photoluminescence (PL) spectra of QDs inside L3 cavity of photonic crystals with a lattice constant of 420 nm. (b) Time resolved emission of XX QD far detuned 120 nm from the cavity after subtracted from the background. The white line is the exponential fit of 2.2 ns while the bottom of the plot shows the residual of fit. Both measurements were performed at 4K.

4. Single photon emitters.

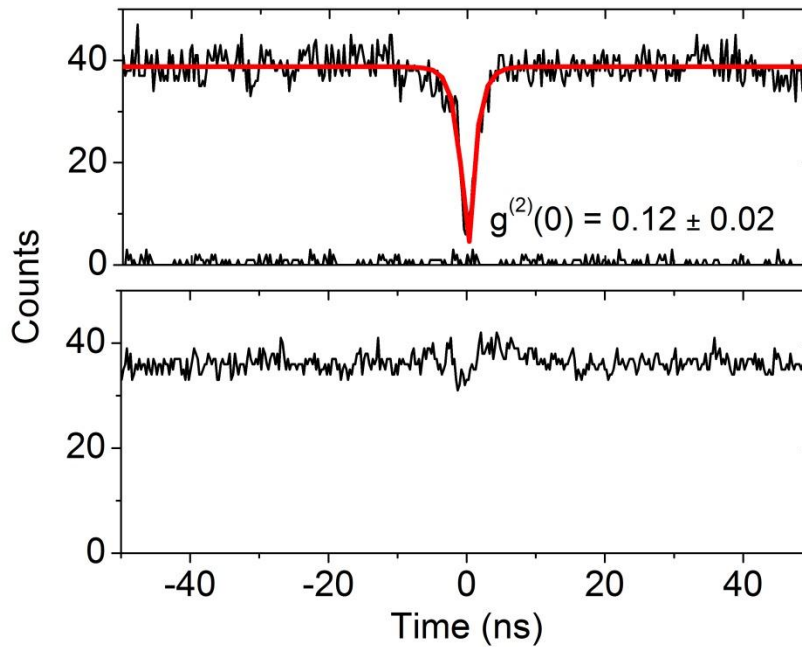


Fig. S5(a) Raw histogram of the second order correlation measurements for the XX emission on resonance with the cavity at 22 K after 6,800s. The bottom curve is the background noise due to the low dark count of SSPD. (b) Raw histogram of the second order correlation measurements for cavity at 4K.

Fig. S5 exhibits the raw histogram of the second order correlation measurements from figure 4 in the manuscript. We fitted the histogram for a single QD in a cavity (Fig. S5(a)) with the same expression as in the manuscript;

$$g^{(2)}(\tau) = 1 - \left[(1 - g^{(2)}(0)) \exp\left(-\frac{|\tau|}{\tau_\sigma}\right) \right] \quad [1]$$

where τ_σ is a time constant assigned to a combination for the emission lifetime and the inverse pumping rate. The fitted $g^{(2)}(0)$ is 0.12 ± 0.02 . This is 0.02 difference with the fitted $g^{(2)}(0)$ from the histogram without background. The small background count is related with the low dark count of the SSPD.

The difference between the temporal width of the second order correlation (with continuous wave excitation) and the lifetime of XX (with pulse excitation) can be explained by the low pumping rate [6, 7]. Santori previously observed a temporal width of 3 ns while the radiative lifetime is 0.5 ns and he explained the difference by a model assuming that the pump process is mainly a two-step process, while electrons and holes are captured independently [6]. Dorenbos *et al.* suggested that the time constant τ_σ is just a sum between the emission lifetime and the inverse pumping rate [7].

In Fig. S5(b), the raw histogram of the second order correlation of the cavity is presented. At the first sight, we observe a bunching with a small narrow antibunching dip in the center. However, the ratio between the signal and the noise (~ 20 times) is much larger than the count fluctuations close to the zero delay (~ 0.16 times). Therefore, we conclude that this histogram shows no antibunching.

References

1. Cade, N. I. *et al.* Optical characteristics of single InAs/InAsP/InP(100) quantum dots emitting at 1.55 μm . *Appl. Phys. Lett.* 89, 181113 (2006).
2. Gong, M., Zhang, W., Han, Z., Guo, G. & He, L. Atomistic pseudopotential calculations of the optical properties of InAs/InP self-assembled quantum dots. *Appl. Phys. Lett.* 99, 231106 (2011).
3. Lund-Hansen T., *et al.*, Experimental realization to highly efficient broadband coupling of single quantum dots to a photonic crystal waveguide, *Phys. Rev. Lett.* 101, 113903 (2008).
4. Lodahl, P., *et al.*, Controlling the dynamics of spontaneous emission from quantum dots by photonic crystals, *Nature*, 430, 654. (2004).
5. Wang, Q., Stobbe, S., and Lodahl, P., Mapping the local density of optical states of a photonic crystal with single quantum dots, *Phys. Rev. Lett.* 107, 167404 (2011).
6. Santori, C. M., Generation of nonclassical light using semiconductor quantum dots, *Stanford Dissertation* (2003).
7. Dorenbos S. *et al.*, Position controlled nanowires for infrared single photon emission, *Appl. Phys. Lett.* 97, 171106 (2010).